

# AP-2 $\gamma$ Induces p21 Expression, Arrests Cell Cycle, and Inhibits the Tumor Growth of Human Carcinoma Cells<sup>1</sup>

Hualei Li, Prabhat C. Goswami and Frederick E. Domann

Free Radical and Radiation Biology Program, Department of Radiation Oncology, The University of Iowa, Iowa City, IA 52242, USA

## Abstract

Activating enhancer-binding protein 2 $\gamma$  (AP-2 $\gamma$ ) is a member of the developmentally regulated AP-2 transcription factor family that regulates the expression of many downstream genes. Whereas the effects of AP-2 $\alpha$  overexpression on cell growth are fairly well established, the cellular effects of AP-2 $\gamma$  overexpression are less well studied. Our new findings show that AP-2 $\gamma$  significantly upregulates p21 mRNA and proteins, inhibits cell growth, and decreases clonogenic survival. Cell cycle analysis revealed that forced AP-2 $\gamma$  expression induced G<sub>1</sub>-phase arrest, decreased DNA synthesis, and decreased the fraction of cells in S phase. AP-2 $\gamma$  expression also led to cyclin D1 repression, decreased Rb phosphorylation, and decreased E2F activity in breast carcinoma cells. AP-2 $\gamma$  binding to the p21 promoter was observed *in vivo*, and the absence of growth inhibition in response to AP-2 $\gamma$  expression in p21 (–/–) cells demonstrated that p21 caused, at least in part, AP-2–induced cell cycle arrest. Finally, the tumor growth of human breast carcinoma cells *in vivo* was inhibited by the expression of AP-2 $\gamma$  relative to empty vector–infected cells, suggesting that AP-2 $\gamma$  acts as a tumor suppressor. In summary, expression of either AP-2 $\gamma$  or AP-2 $\alpha$  inhibited breast carcinoma cell growth; thus, these genes may be therapeutic targets for breast cancer.

*Neoplasia* (2006) 8, 568–577

**Keywords:** AP-2, p21, cell cycle, carcinoma, tumor suppressor.

## Introduction

The family of activating enhancer-binding protein 2 (AP-2) transcription factors consists of five different genes: AP-2 $\alpha$  [1,2], AP-2 $\beta$  [3], AP-2 $\gamma$  [4], AP-2 $\delta$  [5], and AP-2 $\epsilon$  [6]. All AP-2 family members share a high homology and similar multidomain structures consisting of a less-conserved proline-rich transactivation domain, a highly conserved basic helical DNA-binding domain, and a dimerization domain, allowing them to form homodimers and heterodimers [7]. Among various family members, AP-2 $\alpha$  has been more extensively studied than the others. AP-2 $\alpha$  is a retinoic acid–inducible transcription factor that participates in the

proper development of the eyes, face, limbs, body wall, and neural crest [8–10]. Both AP-2 $\alpha$  and AP-2 $\gamma$  are required in early embryonic development and are involved in proliferation and differentiation [11,12].

AP-2 $\alpha$ –regulated genes are involved in many important biologic functions and include genes such as *c-kit* [13], *MUC18* [14], *MMP-2* [15], and *KAI1* [16]. AP-2 $\gamma$  has been reported to participate in the regulation of ErbB2 and estrogen receptor (ER)  $\alpha$ , both of which are implicated in breast cancer initiation and progression [17–19]. AP-2 $\alpha$  overexpression can reduce thymidine synthesis and BrdU incorporation, and can induce hypophosphorylated Rb and the universal cell cycle inhibitor, p21WAF1/CIP1 [20]. In addition to arresting cell cycle progression, AP-2 $\alpha$  was found to induce programmed cell death, and both AP-2 $\alpha$  and AP-2 $\gamma$  are susceptible to caspase 3 cleavage [20,21]. The AP-2 $\alpha$  protein can physically and functionally interact with many other proteins, including p53 [22], retinoblastoma protein (pRb) [23], c-Myc [24], and SV40 large T antigen [1]. Although fewer such studies have been performed on AP-2 $\gamma$  to date, it has been demonstrated to bind p53 in a manner similar to that previously described for AP-2 $\alpha$  [22].

As mentioned above, AP-2 $\alpha$  and AP-2 $\gamma$  are associated with the expression of ER $\alpha$  and ErbB-2 in breast cancer, both of which can promote tumorigenesis and metastasis [17]. By contrast, AP-2 $\alpha$  appears to display tumor-suppressor activity in breast cancer cells, melanoma cells, and prostate cancer cells [13,14,25]. Vascular endothelial growth factor, an angiogenic factor in cancer development, was found to be deregulated after AP-2 $\alpha$  expression [25]. A metastasis inhibitor, KiSS-1, was also demonstrated to be induced by AP-2 $\alpha$  in breast cancer cell lines [26]. Low nuclear AP-2 $\alpha$  expression in human breast cancer was found to be associated with disease progression and an increased metastatic capability of the tumor [27]. Reduced nuclear AP-2 expression was also demonstrated to

Abbreviations: AP-2, activating enhancer-binding protein 2; PCR, polymerase chain reaction; pRB, retinoblastoma protein; PBS, phosphate-buffered saline; MOI, multiplicity of infection. Address all correspondence to: Frederick E. Domann, Free Radical and Radiation Biology Program, University of Iowa, B180 ML, Iowa City, IA 52242.  
E-mail: [frederick-domann@uiowa.edu](mailto:frederick-domann@uiowa.edu)

<sup>1</sup>This work was supported by National Institutes of Health grants R01 CA73612, CA66081, and CA111365.

Received 10 May 2006; Revised 2 June 2006; Accepted 6 June 2006.

Copyright © 2006 Neoplasia Press, Inc. All rights reserved 1522-8002/06/\$25.00  
DOI 10.1593/neo.06367

independently predict an elevated risk of recurrent disease in breast cancer [28]. Additionally, AP-2 $\alpha$  is a target of DNA methylation-mediated silencing in human breast cancer cells [29], whereas AP-2 $\gamma$  is reported to be a marker of germ cell tumors [30,31]. A recent study [32] revealed that there is a dual role for AP-2 $\gamma$  in different mammary tumorigenic stages: inhibition of tumor initiation and promotion of proliferation. Taken together, these findings provide evidence that AP-2 participates in a complex biologic dynamics, including cell cycle progression, apoptosis, and tumor formation.

The tumor-suppressor activity of AP-2 $\alpha$  was shown by demonstrating that its forced expression led to decreased cancer cell growth *in vivo* and *in vitro* [15,20]. Because AP-2 $\alpha$  and AP-2 $\gamma$  share a high homology and certain common biologic functions, including heterodimer formation, it is of considerable interest to determine whether AP-2 $\gamma$  acts in a manner similar to that of AP-2 $\alpha$  regarding cell growth regulation. Thus, we performed experiments to determine whether AP-2 $\gamma$  may similarly act as a tumor suppressor in human carcinoma cells.

Our data compared AP-2 $\alpha$  and AP-2 $\gamma$  in several aspects related to human cancer cell growth. We used recombinant adenoviruses Ad-AP-2 $\alpha$  and Ad-AP-2 $\gamma$  to elevate wild-type (wt) AP-2 $\alpha$  and AP-2 $\gamma$  expression, respectively, and measured the effects of forced AP-2 expression in human carcinoma cells. Our results indicated that wt AP-2 $\alpha$  or AP-2 $\gamma$  overexpression inhibited MDA MB-231 cell growth, decreased clonogenic survival, and arrested cell cycle progression. Both AP-2 $\alpha$  and AP-2 $\gamma$  induced p21 mRNA and protein to the same level within 24 hours of adenovirus infection. Similar effects on cyclin D1, E2F, and Rb phosphorylation were observed in both treatments. AP-2 $\alpha$  and Ad-AP-2 $\gamma$  share the same DNA consensus-binding site; thus, it may not be surprising that AP-2 $\gamma$  was enriched at the AP-2-binding sites in the p21 promoter [33]. Taken together, these findings strongly suggest that these two AP-2 family members perform their functions through similar pathways, perhaps even working in concert. The failure of Ad-AP-2 expression to arrest cell cycle in p21 knockout cells revealed the importance of p21 in both AP-2 $\alpha$ - and AP-2 $\gamma$ -induced cell cycle arrests. In our *in vivo* animal experiments, both AP-2 $\alpha$  and AP-2 $\gamma$  significantly decreased MDA MB-231 tumorigenicity and inhibited tumor growth in nude mice. Thus, AP-2 may function as a tumor suppressor in human breast cancer.

## Materials and Methods

### Cell Culture

MDA MB-231 human breast adenocarcinoma cells were obtained from the American Type Culture Collection (Rockville, MD). They were routinely cultured in RPMI 1640 medium. HCT116 parental and p21 (-/-) cells (kindly provided by Dr. Bert Vogelstein) were kept in Dulbecco's modified Eagle's medium. All media were supplemented with 10% fetal bovine serum and 50  $\mu$ g/ml penicillin/streptomycin. Cells were incubated at 37°C with 95% air and 5% CO<sub>2</sub>. The medium was changed every 3 to 4 days.

### Adenovirus Constructs

AP-2 $\alpha$  cDNA (provided by Dr. Trevor Williams [2]) was subcloned into a pcDNA3 mammalian expression vector (Invitrogen, Carlsbad, CA). The AP-2 $\gamma$  expression vector AP-2 $\gamma$  pcDNA3 was generously provided by Dr. Ronald J. Weigel [19]. Ad-AP-2 $\alpha$  and Ad-AP-2 $\gamma$  adenoviruses were produced at the University of Iowa's Gene Transfer Vector Core Facility. The corresponding vector control was Ad-Bgl II, which contains only the adenovirus backbone. All adenovirus stocks were maintained at the University of Iowa's Vector Core Facility, where infectious particles were also amplified, purified, and characterized.

### Clonogenic Survival Assay

We infected MDA MB-231 cells with 100 multiplicity of infection (MOI) of Ad-Bgl II, Ad-AP-2 $\alpha$ , or Ad-AP-2 $\gamma$ . Twenty-four hours after infection, the total number of cells was determined using a Coulter counter (Beckman Coulter, Inc., Fullerton, CA). The number of cells plated into each cell culture dish was adjusted to give about 50 to 100 surviving colonies per dish. The cells were incubated at 37°C for 14 days to form colonies. The colonies were then fixed and stained by gentle addition of crystal violet to the medium in the cell culture dish. Colonies containing more than 50 cells were counted as surviving clonogenic cells, and the surviving fraction was normalized to the plating efficiency, as given below

$$\text{Plating efficiency (PE)} = \frac{\text{colonies formed}}{\text{untreated cells seeded}}$$

$$\text{Surviving efficiency (SE)} = \frac{\text{colonies formed}}{\text{number of cells seeded} \times \text{PE}}$$

### Nuclear Protein Extraction

Nuclear extracts were prepared according to the method of Zhu et al. [34], as previously described. Briefly, the medium was removed from tissue culture dishes. Cells were washed twice with phosphate-buffered saline (PBS) and scraped-harvested in 500  $\mu$ l of ice-cold hypotonic buffer (10 mM HEPES, 1.5 mM MgCl<sub>2</sub>, 10 mM KCl, and 0.5 mM DTT). Cells were incubated on ice for 20 minutes, lysed by a glass dounce homogenizer with type B pestle, and centrifuged at 300g for 5 minutes. Supernatants were saved as cytosolic proteins, and 40  $\mu$ l of ice-cold high-salt buffer (20 mM HEPES, 25% glycerol, 0.42 M NaCl, 1.5 mM MgCl<sub>2</sub>, 0.2 mM EDTA, 0.5 mM PMSF, and 0.5 mM DTT) was added to the nuclear pellets and mixed. The nuclei were incubated on ice for 15 minutes and centrifuged at maximum speed for 1 minute. Supernatants were saved as nuclear protein extracts. Protein concentrations were determined with Bio-Rad DC protein assay (Bio-Rad Laboratories, Hercules, CA), according to the manufacturer's instructions.

### Total Protein Extraction

Cells were collected by trypsinization and centrifugation and incubated in RIPA buffer [150 mM NaCl; 50 mM Tris, pH 8.0; 1 mM EDTA; 0.5% NP40; 0.1 mM Na<sub>3</sub>VO<sub>4</sub>; 1% sodium deoxycholic acid; and 0.1% sodium dodecyl sulfate

(SDS)] for 30 minutes on ice. After 15 seconds of sonication, cell lysates were centrifuged for 1 minute at 13,000 rpm. Supernatants were saved as total protein extracts.

#### Western Blot Analysis

Equal amounts of proteins from differently treated cells were size-fractionated on a 10% (pRb) or a 12% (all other proteins) Tris–HCl polyacrylamide ready gel (Bio-Rad Laboratories). Separated proteins were then electrotransferred to a nitrocellulose membrane (Schleicher and Schuell, Keene, NH) by running at 100 V for 1 hour (6 hours for pRb). For AP-2 $\alpha$  and AP-2 $\gamma$  Western blot analyses, the primary antibodies were mouse anti-AP-2 $\alpha$  IgG and mouse anti-AP-2 $\gamma$ -IgG, respectively (Santa Cruz Biotechnology, Santa Cruz, CA), both used at 1:400 dilution. For p21 Western blot analyses, the primary antibody was mouse anti-p21 IgG (PharMingen, San Diego, CA), used at a dilution of 1:250. For phospho-Rb (pS780) Western blot analyses, the primary antibody was rabbit anti-pRb (pS780) IgG (Cell Signaling Technology, Beverly, MA), used at a dilution of 1:1000. For cyclin D1 Western blot analyses, the primary antibody was mouse anti-cyclin D1 IgG (PharMingen), used at a dilution of 1:1500. For  $\beta$ -actin Western blot analyses, the primary antibody was mouse anti-human  $\beta$ -actin IgG (Santa Cruz Biotechnology), used at a dilution of 1:3000. For AP-2, cyclin D1, and actin Western blot analyses, the secondary antibody was goat anti-mouse IgG (PharMingen), used at a 1:10,000 dilution. For p21 and pRb (pS780), the secondary antibody was used at 1:3000 dilution. Blots were washed with TTBS (0.02 M Tris–HCl buffer, pH 7.5; 0.137 M NaCl; and 0.1% Tween 20). Detection by chemiluminescence reaction was carried out using an enhanced chemiluminescence kit (Amersham Pharmacia Biotech, Piscataway, NJ), followed by exposure to Kodak X-ray film (Kodak, Rochester, NY).

#### Electrophoretic Gel Mobility Shift Assay (EMSA)

We used double-stranded oligodeoxynucleotides containing a consensus AP-2-binding sequence (Promega, Madison, WI). The probe was made by labeling these double-stranded oligonucleotides with [ $\gamma$ - $^{32}$ P] ATP using T4 polynucleotide kinase. After that, 10  $\mu$ g of nuclear protein was incubated with the  $^{32}$ P-radiolabeled oligonucleotide probe in the presence of 1  $\mu$ g of poly(dIdC) (Amersham Pharmacia Biotech) and 1 $\times$  gel shift buffer (10 mM Tris, pH 7.5; 50 mM NaCl; 1 mM MgCl<sub>2</sub>; 0.5 mM EDTA; 0.5 mM dithiothreitol; and 4% glycerol) at room temperature for 20 minutes. Binding reactions were loaded onto a 5% polyacrylamide gel and run at 100 V in 1 $\times$  TBE (90 mM Tris, 90 mM boric acid, and 2 mM EDTA, pH 8.0). The gels were wrapped in plastic wrap and exposed to Kodak X-ray film overnight at  $-80^{\circ}\text{C}$ . To assess the specificity of the binding reaction, antibodies specific to AP-2 $\alpha$  and AP-2 $\gamma$  were incubated with each binding reaction for 20 minutes before loading onto the gel.

#### Plasmid Constructs and Reporter Gene Assays

An E2F-responsive reporter construct, pE2F-Luc (Clontech, Mountain View, CA), containing four E2F consensus-

binding sites in the enhancer region upstream of the *firefly luciferase* gene was used to characterize E2F-transactivating activity in cells expressing AP-2. Firefly luciferase activities were determined using the Dual Luciferase assay system (Promega) and were normalized relative to renilla luciferase activity. Reproducibility was ensured by transfection performed in triplicate.

#### Cell Cycle Analysis

Cells were plated at  $5 \times 10^5$  cells/dish and infected with 100 MOI of various adenoviruses for 24 hours. After 24-hour infection, the medium was changed, and cells were pulse-labeled with BrdU (final concentration, 1  $\mu$ M) for 30 minutes. Cells were washed with 1 $\times$  PBS and fixed with 70% cold ethanol. Cells were washed with PBT (1 $\times$  PBS, 1 mg/ml BSA, and 0.1% Tween 20) on the next day and digested with pepsin for half an hour. After neutralization with 0.1 M borax, nuclei were washed again and incubated with BrdU primary antibody (Becton Dickinson Immunocytometry Systems, San Jose, CA) and fluorescein isothiocyanate (FITC) GAM secondary antibody (Becton Dickinson), following the manufacturer's protocol. Samples were analyzed at the Flow Cytometry Facility at the University of Iowa. Data were analyzed with CellQuest software (Becton Dickinson) for combined BrdU/propidium iodide (PI) staining, and with ModFit software (Verity Software House, Topsham, ME) for PI staining only.

#### Real-Time Reverse Transcription–Polymerase Chain Reaction (RT-PCR) Analysis

Total RNA was extracted using Qiagen RNeasy kit (Qiagen, Inc., Valencia, CA). RT was performed using high-capacity cDNA archive kit (Applied Biosystems, Foster City, CA), according to the manufacturer's protocol. PCR conditions were as follows:  $95^{\circ}\text{C}$  for 10 minutes, followed by 40 cycles of denaturation at  $95^{\circ}\text{C}$  for 30 seconds, and annealing and extension at  $60^{\circ}\text{C}$  for 1.5 minutes. PCR was performed, and data were collected using the ABI Prism 7000 real-time sequence detection system (Applied Biosystems). The target gene was detected using SYBR green PCR master mix (Applied Biosystems). Differences in expression were determined using relative quantity calculated by standard curve. p21 mRNA level was determined by SYBR Green master mix (Applied Biosystems) using forward primer 5'-ATCCCGTGTCTCCTTT and reverse primer 5'-GCTGGCATGAAGCC. Cyclin D1 was detected by using the forward primer 5'-GAGGTCTGCGAGGAACAGAAGT and the reverse primer 5'-CCTTCATCTTAGAGGCCACGA.

#### Chromatin Immunoprecipitation (ChIP) Assays

MDA MB-231 cells were infected with 100 MOI of Ad-Bgl II, Ad-AP-2 $\alpha$ , or Ad-AP-2 $\gamma$  for 24 hours. Cells were treated with 1% formaldehyde for 10 minutes. The cells were then gently scraped and collected by centrifugation at  $4^{\circ}\text{C}$ . Cells pellets were resuspended in 500  $\mu$ l of sonication buffer (50 mM Tris–Cl, pH 8.0; 10 mM EDTA; 1% SDS; and proteinase inhibitors) and incubated on ice for 10 minutes. DNA–protein complexes were sonicated to lengths between 200 and 1000 bp, as determined by gel electrophoresis. Samples

were centrifuged at 16,000g at 4°C to spin out cell debris, and then the supernatant was diluted 10-fold with ChIP dilution buffer. One tenth of the sample was set aside for input control, and the remaining sample was precleared with protein A/G PLUS Agarose (Upstate Biotech, Charlottesville, VA). Following preclearing, the sample was split in half and the two portions were incubated with 30  $\mu$ l of anti-AP-2 $\alpha$  antibody (Santa Cruz Biotechnology) and 30  $\mu$ l of anti-AP-2 $\gamma$  antibody (Santa Cruz Biotechnology), respectively, plus protein A/G PLUS agarose. Following overnight incubation at 4°C, the beads were washed with low-salt, high-salt, and LiCl wash buffers, and then twice with Tris-EDTA, pH 8.0. Chromatin-antibody complexes were eluted, and DNA-protein cross-links were reversed with 0.4 M NaCl (final concentration) at 65°C for 4 hours. Samples were subsequently treated with proteinase K, and genomic DNA was recovered by Qiagen DNeasy kit (Qiagen, Inc.) and quantitated with a BioPhotometer (Eppendorf Scientific, Hamburg, Germany).

Conventional genomic PCR was used to analyze ChIP DNA using PCR Master Mix (Qiagen, Inc.) following manufacturer's protocol (20% Q-solution was added). PCR was carried out on 70 ng of ChIP DNA using the following conditions: 95°C for 15 minutes, 94°C for 30 seconds, 57°C for 30 seconds, and 72°C for 30 seconds (40 cycles in total). The corresponding PCR primers used were as follows: p21 forward primer 5'-GCCAGATTTGGCTCACTTCG and p21 reverse primer 5'-ACGCTTGGCTCGGCTCTGG.

#### *In Vivo* Tumorigenicity Assays

All animal experiments were conducted in strict accordance with an approved IACUC protocol from the Office of Animal Research at the University of Iowa. Athymic nude mice were housed in specific pathogen-free conditions at the animal care facility at the University of Iowa. Under sterile conditions in a laminar flow hood, 7- to 8-week-old female nude mice were injected subcutaneously with  $5 \times 10^6$  MDA MB-231 cells into each flank. The animals were examined every 4 days for the status of tumor growth. Tumor sizes (Tumor volume = length  $\times$  width  $\times$  height / 2) were measured as a function of time. Animals were sacrificed when any tumor reached 1 cm<sup>3</sup>. To determine the tumorigenic capability of differently treated cells, MDA MB-231 cells were infected with 100 MOI of vector control or Ad-AP-2 for 24 hours before injection into mice. To infect established tumors in mice,  $1 \times 10^9$  pfu of adenoviruses was injected into each tumor when the average diameter was 3 to 4 mm. Animals were grouped at the beginning to achieve the same average tumor volume within each group. Adenoviral injections were performed every 5 days (a total of three times).

## Results

### *Forced Expression of Either AP-2 $\alpha$ or AP-2 $\gamma$ Caused Increased AP-2 DNA-Binding Activity and Decreased Clonogenic Survival*

Some experimental evidence has suggested that AP-2 $\alpha$  is able to inhibit tumor cell growth and thus is a possible

tumor suppressor [13,15]. We selected MDA MB-231 cells (breast carcinoma cell line) to do the following experiments because of its AP-2 $\alpha$ -null expression and low-AP-2 $\gamma$  expression. To demonstrate the effects of AP-2 on MDA MB-231 cells, we used Ad-AP-2 $\alpha$  and Ad-AP-2 $\gamma$  to increase AP-2 $\alpha$  and AP-2 $\gamma$  protein level, respectively. At 24 hours after Ad-AP-2 infection, AP-2 $\alpha$  and AP-2 $\gamma$  expressions were greatly increased in MDA MB-231 cells, in comparison with untreated and Ad-Bgl II-infected cells [35]. Moreover, we demonstrated that overexpressed AP-2 $\alpha$  and AP-2 $\gamma$  bound AP-2 consensus-binding sites (Figure 1A) and were supershifted by their respective AP-2 antibodies (Figure 1A, lanes 7 and 11). MDA MB-231 is an aggressive growing cell line. After introducing AP-2 $\alpha$  or AP-2 $\gamma$  expression by AP-2 adenoviral infection at 100 MOI, the growth rates of MDA

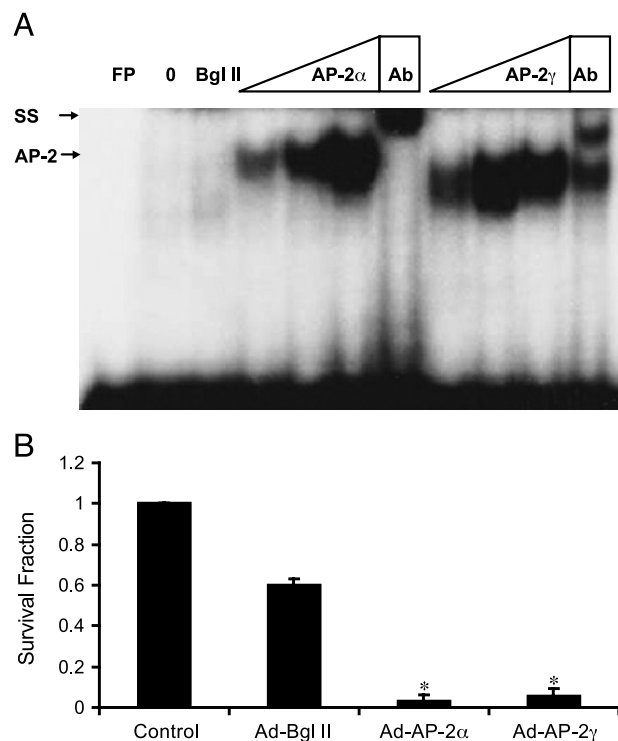


**Figure 1.** Ad-AP-2 $\alpha$  and Ad-AP-2 $\gamma$  adenovirus-infected MDA MB-231 cells showed increased AP-2 DNA-binding activity and decreased clonogenic survival. (A) MDA MB-231 cells were infected with increasing MOI of AP-2 adenoviruses, as indicated by ramps. Nuclear proteins were isolated 24 hours after infection. EMSAs were performed on nuclear extracts of both MDA MB-231 cells to establish AP-2 DNA-binding activity to an AP-2 consensus-binding site *in vitro*. Radiolabeled AP-2 consensus-binding sites were incubated with nuclear extracts under the following different conditions: lane 1: probe only; lane 2: untreated MDA MB-231 nuclear extract; lane 3: vector control Ad-Bgl II-treated cell extract; lanes 4 to 7: extracts from Ad-AP-2 $\alpha$ -treated cells with increasing MOI from 50, 100, 200, and 200; lanes 8 to 11: extracts from Ad-AP-2 $\gamma$ -treated cells with increasing MOI from 50, 100, 200, and 200. To evaluate the specificity of this interaction, antibodies specific to AP-2 $\alpha$  (lane 7) and AP-2 $\gamma$  (lane 11) were incubated with nuclear extracts from 200 MOI of Ad-AP-2-infected MDA MB-231 cells. (B) MDA MB-231 cells ( $2 \times 10^6$ ) were plated in 100-mm dishes and infected with 100 MOI of Ad-Bgl II or Ad-AP-2. After 24-hour infection, cells were trypsinized and subcultured into 60-mm dishes at 500 cells/dish to determine clonogenic fractions. Surviving fractions were normalized to untreated cells. \* $P < .05$  compared to untreated control cells and Ad-Bgl II-treated cells.

MB-231 cells were significantly decreased [35], similar to observations in the literature [20,33]. Moreover, their clonogenic capabilities were lost in 100 MOI of Ad-AP-2–infected MDA MB-231 cells, in comparison with untreated and vector control–treated cells (Figure 1B).

#### Not Only AP-2 $\alpha$ But Also AP-2 $\gamma$ Overexpression Arrested Cell Cycle and Elevated Levels of p21 Protein and mRNA

Cell cycle arrest is one of the mechanisms that could lead to our observations. We performed BrdU incorporation to monitor DNA synthesis during cell division and PI staining for DNA content. Experiments were independently carried out thrice. The cell fractions in G<sub>1</sub>/G<sub>0</sub>, S, and G<sub>2</sub>/M phases were analyzed using CellQuest software (Becton Dickinson). There was a dramatically increased cell number arrested in G<sub>1</sub>/G<sub>0</sub> phase and a significant decrease in the fraction of cells in S phase after a 24-hour Ad-AP-2 $\alpha$  or Ad-AP-2 $\gamma$  infection (Figure 2A).

It has been previously reported that p21 can be induced by AP-2 $\alpha$  and can inhibit cell growth [33]. Western blot analysis and RT-PCR were performed to detect p21 expression after either AP-2 $\alpha$  or AP-2 $\gamma$  expression. AP-2 $\gamma$  caused an upregulation of both p21 mRNA and protein levels in a manner similar to that in AP-2 $\alpha$ . The magnitude of the p21 mRNA increase was about the same in both Ad-AP-2 $\alpha$ – and Ad-AP-2 $\gamma$ –infected cells (Figure 2, C and D).

#### Forced AP-2 Expression Significantly Decreased RB Phosphorylation, Cyclin D1 mRNA and Protein Levels, and E2F-Transactivating Activity

To gain further insight into the mechanism by which AP-2 causes cell cycle arrest, we proceeded to assess other important factors involved in cell cycle progression. Cyclin D1 is one of these factors because it promotes cell cycle progression and is overexpressed in human breast cancers [36–38]. In MDA MB-231 cells, forcing the overexpression of AP-2 $\alpha$  or AP-2 $\gamma$  for 24 hours significantly reduced the steady-state cyclin D1 mRNA level (Figure 3A). Cyclin D1 protein levels were also decreased by AP-2 not only in MDA MB-231 cells but also in HCT116 (human colon carcinoma) cells (Figure 3B). pRb is another major protein that regulates cell cycle transitions from G<sub>1</sub> to S phase. Moreover, changes in p21 and cyclin D1 protein level can affect the phosphorylation status of pRb [39]. Significantly decreased phosphorylated Rb (Ser780, a cyclin D/CDK4–phosphorylated site) was detected by Western blot analysis in Ad-AP-2 $\alpha$ – and Ad-AP-2 $\gamma$ –infected MDA MB-231 cells (Figure 3C). However, there was no change in Rb mRNA levels (data not shown). Another downstream effector in cell cycle progression is the family of E2F transcription factors. Elevated E2F transactivation is a key event during G<sub>1</sub>–S cell cycle transition. We used an E2F-responsive luciferase reporter, which contains four E2F-binding sites fused to the *firefly luciferase* gene, to measure E2F function after AP-2 overexpression in MDA MB-231 cells. Relative luciferase activity (firefly luciferase/renilla luciferase) was significantly decreased in AP-2–expressing cells compared with vector control–infected and untreated cells (Figure 3D).

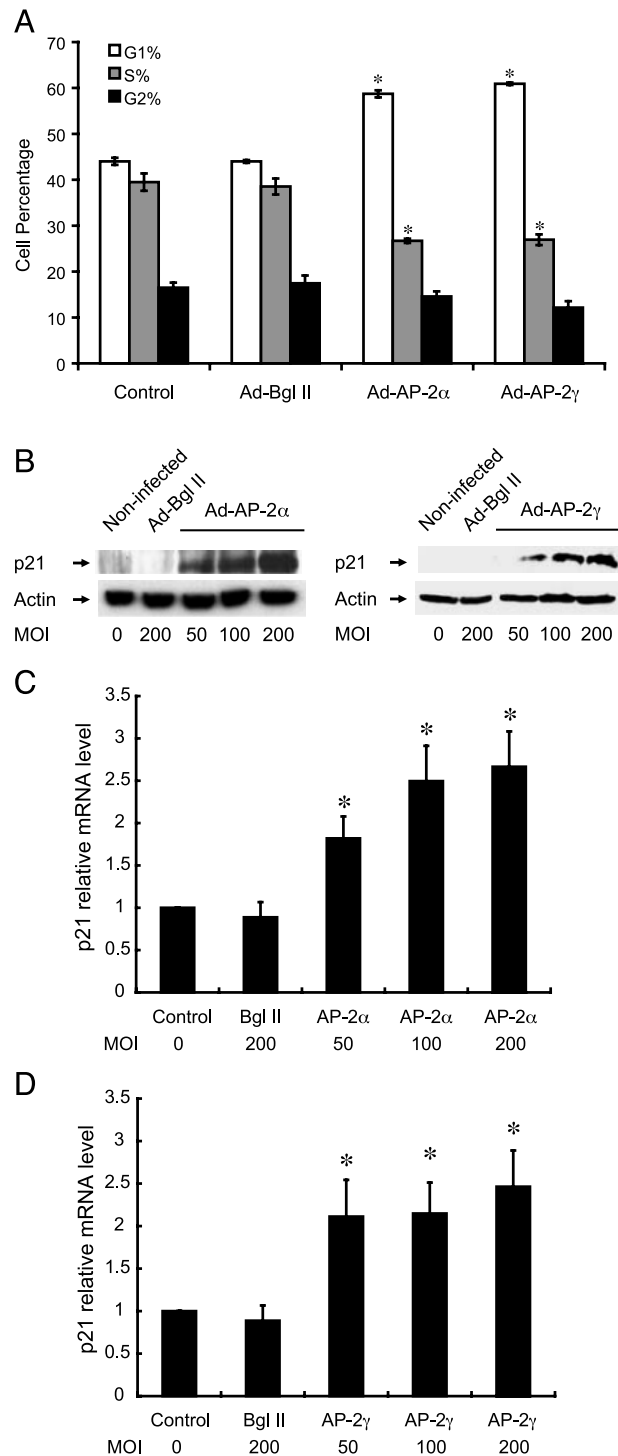


**Figure 2.** Not only AP-2 $\alpha$  but also AP-2 $\gamma$  overexpression arrested cell cycle and elevated p21 protein and mRNA levels in MDA MB-231 cells. (A) MDA MB-231 cells were plated and infected with 100 MOI of various adenoviruses, as indicated. After 24-hour incubation, cells were pulsed with BrdU and labeled with BrdU antibody, and flow cytometry was performed. The fractions of the cell population in different phases of the cell cycle were analyzed using CellQuest Software. (B) MDA MB-231 cells were infected with various MOI adenoviruses. Nuclear proteins and total RNA were isolated 24 hours after infection. Western blot analyses were carried out to determine p21 protein levels.  $\beta$ -Actin was used as the control for loading and transfer. (C and D) MDA MB-231 cells were treated as described in (B). Total mRNA was isolated 24 hours after infection. Quantitative RT-PCR was used to determine steady-state p21 mRNA levels. Results are expressed as mean  $\pm$  SEM ( $n = 3$ ). \* $P < .05$  compared to untreated and vector control–treated mRNA samples. <sup>†</sup> $P < .05$  compared to vector control–treated cells.

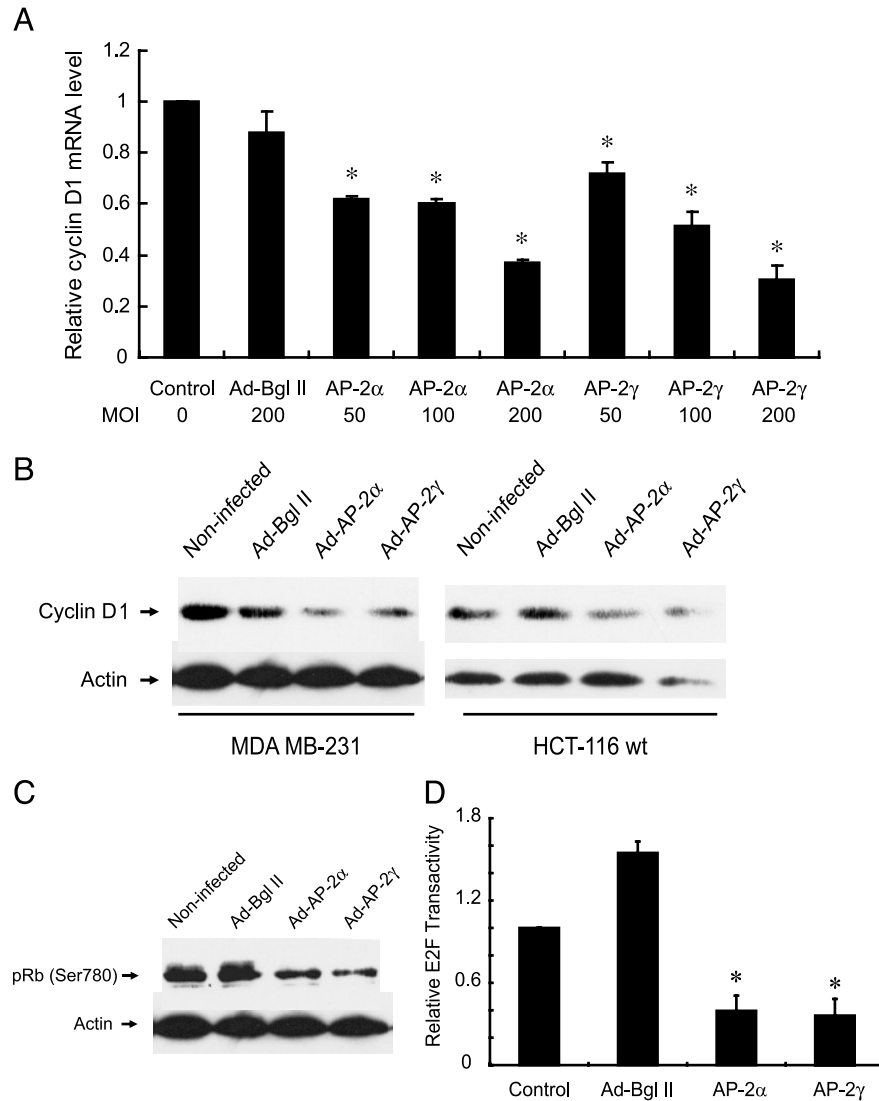


**Figure 3.** Forced AP-2 expression significantly decreased Rb phosphorylation, cyclin D1 mRNA and protein levels, and E2F responsive promoter activity. (A) Cells were infected with vector control or Ad-AP-2, as indicated. Total mRNA was harvested 24 hours after infection. Quantitative RT-PCR was used to determine cyclin D1 mRNA level in MDA MB-231 cells. Results are expressed as mean  $\pm$  SEM ( $n = 3$ ). \*  $P < .05$  compared to untreated and vector control–treated mRNA sample. (B) Cells were infected with 100 MOI of vector control or Ad-AP-2. Total cell lysates were harvested 24 hours after infection. Western blot analyses were conducted to determine cyclin D1 protein levels in both MDA MB-231 and HCT116 wt cells.  $\beta$ -Actin was used as a control for loading and transfer. (C) Cells were treated as described above (B). Western blot analyses were conducted to determine pRb (S780) protein level in MDA MB-231 cells. (D) MDA MB-231 cells were infected with Ad-Bgl II, Ad-AP-2 $\alpha$ , or Ad-AP-2 $\gamma$  at 100 MOI and transfected with 5  $\mu$ g of 4 $\times$  E2F firefly luciferase reporter and 1  $\mu$ g of Cytomegalovirus renilla luciferase reporter, as described in the Materials and Methods section. Total proteins from adherent cells were collected, and firefly luciferase activities were measured 24 hours after infection. \* $P < .05$  compared with control and vector control–treated cells.

#### Overexpression of AP-2 $\alpha$ or AP-2 $\gamma$ Failed to Cause G<sub>1</sub> Arrest and to Inhibit BrdU Incorporation in p21 (–/–) Cells

p21, a well-known tumor suppressor, is upregulated by AP-2 $\alpha$  and AP-2 $\gamma$  and may mediate, at least in part, the observed AP-2–induced cell cycle arrest. To determine whether AP-2 caused cell cycle arrest through p21, we analyzed differences in cell cycle distribution and DNA synthesis after AP-2 treatment in HCT116 parent (p21 wt) cells and HCT116 p21 (–/–) cells. First, we confirmed whether p21 protein was increased in HCT116 wt cells after AP-2 overexpression and whether there was no detectable p21 protein in either untreated and Ad-AP-2–treated HCT116 p21 (–/–) cells (Figure 4A). We found that BrdU incorporation, an indicator of S-phase DNA synthesis, was significantly

decreased in both Ad-AP-2 $\alpha$ – and Ad-AP-2 $\gamma$ –infected cells compared with noninfected and Ad-Bgl II–infected HCT116 wt cells; however, there was no decrease observed in HCT116 p21 (–/–) cells (Figure 4B). PI staining showed an elevated fraction of cells in G<sub>1</sub>/G<sub>0</sub> phase and a decreased fraction of cells in S phase in both Ad-AP-2 $\alpha$ – and Ad-AP-2 $\gamma$ –infected HCT116 parent cells compared with noninfected and Ad-Bgl II–infected HCT116 parental cells (Figure 4C). These results were consistent with those previously obtained in the MDA MB-231 cell line (Figure 3). In contrast to HCT116 parent cells, there was no decrease in S-phase fraction and no increase in G<sub>1</sub>-phase fraction between vector control–infected and Ad-AP-2 $\alpha$ – and Ad-AP-2 $\gamma$ –infected HCT116 p21 (–/–) cells with the same MOI (Figure 4D).

The general pattern of cell cycle distribution after Ad-AP-2 infection was not as pronounced in HCT116 p21 (-/-) cells as in HCT116 wt cells. As to untreated HCT116 wt and p21 (-/-) cells, they displayed quite different cell cycle distributions, suggesting that knocking out p21 has effects on elevating cell percentage in S phase while decreasing G<sub>1</sub>-phase fraction (Figure 4D). It was noted that there were both reduced G<sub>1</sub>/G<sub>0</sub> fraction and enhanced G<sub>2</sub>/M percentage in any adenovirally infected p21 (-/-) cell. The appearance of G<sub>2</sub> arrest might be due to the unavailability of p21-mediated G<sub>1</sub> arrest after adenoviral infection, which leads to both arrests. Taken together, results from this series of experiments indicated that p21 is a major player involved in AP-2-induced cell cycle inhibition in human carcinoma cells.

#### Both AP-2 $\alpha$ and AP-2 $\gamma$ Bind to the p21 Proximal Promoter Region *In Vivo*

It has been reported that AP-2 $\alpha$  binds to p21 proximal promoter and activates p21 expression [33]. AP-2 $\alpha$  recombinant protein was demonstrated to bind DNA oligonucleotides designed from the p21 promoter *in vitro* [33]. AP-2 family members, including AP-2 $\gamma$ , can interact with the same DNA consensus-binding sites and can activate many genes. To determine whether AP-2 $\alpha$  and AP-2 $\gamma$  can bind to

the identified AP-2-binding sites on the p21 proximal promoter in MDA MB-231 cells *in vivo*, we used ChIP. We observed the enrichment of both AP-2 $\alpha$  and AP-2 $\gamma$  on the p21 promoter in the respective adenovirus-infected cells (Figure 5). Although the amount of input DNA was equivalent, only the ChIP DNA from the Ad-AP-2-infected cells yielded a PCR product, indicating that AP-2 was bound to the p21 promoter *in vivo*.

#### AP-2 Expressing MDA MB-231 Cells Showed Less Tumorigenicity, and Adenoviral AP-2 Infection Significantly Delayed the Growth of Established Tumors *In Vivo*

To further investigate the tumor-suppressing role of AP-2 $\alpha$  and AP-2 $\gamma$  *in vivo*, we monitored the tumor-forming ability and growth rates of differently treated cells in nude mice. In the first experiment, MDA MB-231 cells were infected with 100 MOI of Ad-Bgl II or Ad-AP-2 $\alpha$  or Ad-AP-2 $\gamma$  for 24 hours *in vitro*. Five million cells from different groups were injected into each flank. The mice injected with untreated and vector control-treated cells were sacrificed because they reached the maximum tumor size when the tumor with Ad-AP-2 $\alpha$ - or Ad-AP-2 $\gamma$ -infected cells had just started to grow. The recorded tumor initiation times of Ad-AP-2 $\alpha$ - or Ad-AP-2 $\gamma$ -infected cells were significantly later

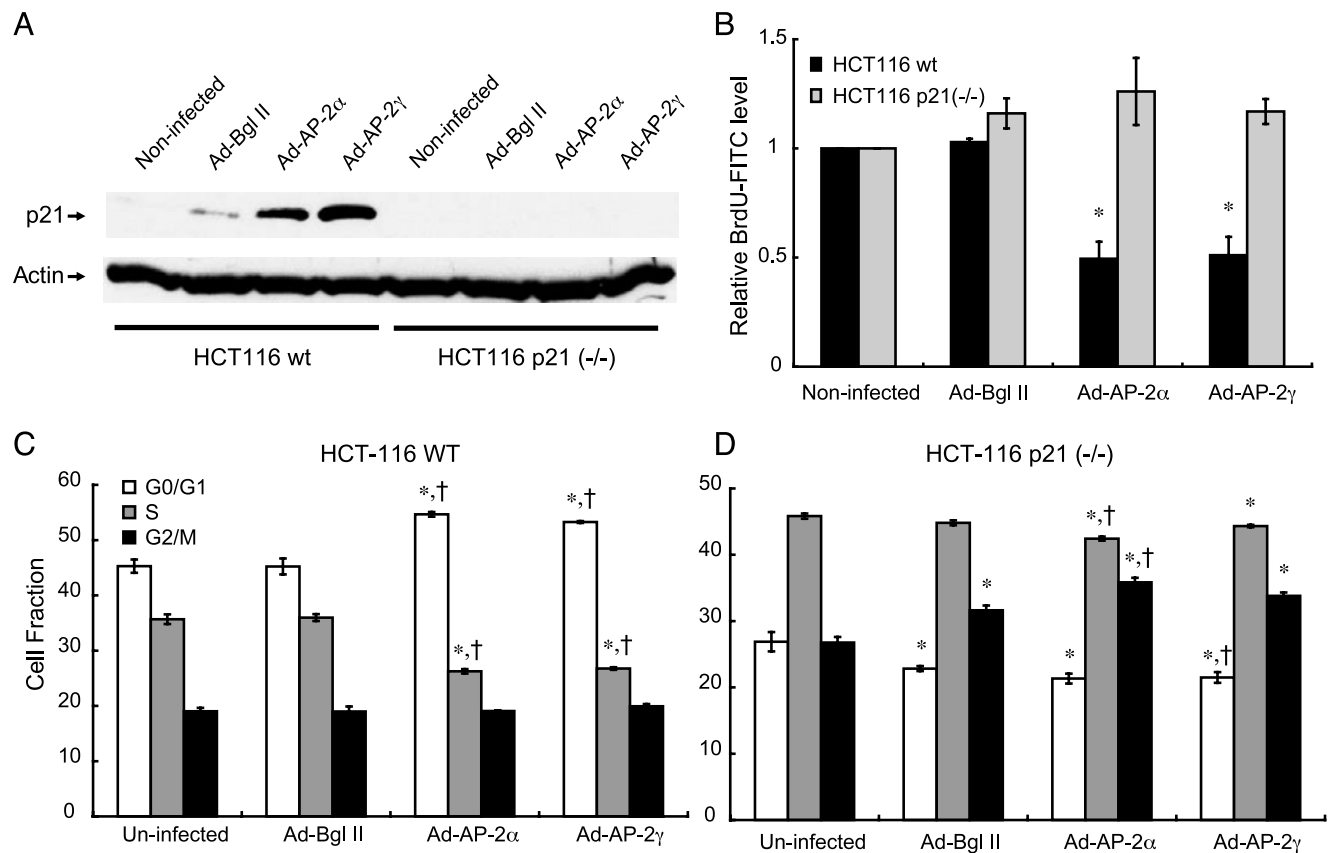


**Figure 4.** Overexpression of AP-2 $\alpha$  or AP-2 $\gamma$  failed to induce p21 protein G<sub>1</sub> arrest and to inhibit BrdU incorporation in HCT116 p21 (-/-) cells. HCT116 parent and p21 (-/-) cells were infected with 100 MOI of vector control or Ad-AP-2 for 24 hours. (A) Total proteins were isolated, and Western blot analysis was carried out to detect p21 protein level.  $\beta$ -Actin was used as control for loading and transfer. (B) Cells were pulsed with BrdU and labeled with BrdU antibody. PI staining was used to detect total DNA content. Flow cytometry was carried out. Quantitative BrdU FITC level was calculated for every cell group. \* $P < .05$  compared to untreated control cells and vector control-treated cells. Fractions of cells are shown as histograms of HCT116 wt cells (C) and HCT116 p21 (-/-) cells (D). \* $P < .05$  compared to untreated control cells. † $P < .05$  compared to vector control-treated cells.

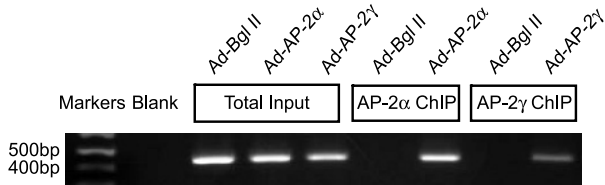


**Figure 5.** Both AP-2 $\alpha$  and AP-2 $\gamma$  bind to p21 proximal promoter *in vivo*. MDA MB-231 cells were infected with vector control, Ad-AP-2 $\alpha$ , or Ad-AP-2 $\gamma$  at 100 MOI. Twenty-four hours after infection, AP-2 $\alpha$  and AP-2 $\gamma$  antibodies were used to immunoprecipitate protein-bound DNA. An equivalent amount of genomic DNA without immunoprecipitation was used as input control. Standard PCR was carried out to determine the extent of AP-2 binding to the p21 proximal promoter region illustrated in Zeng et al. [33].

than those of untreated and vector control-treated cells (Figure 6A). The survival of animals was greatly improved in animals bearing Ad-AP-2-infected cells (data not shown). Compared with both controls, it took approximately 1 month longer to reach the same tumor size for Ad-AP-2-infected tumors. To determine whether there was an effective therapeutic response in establishing tumors treated with Ad-AP-2 adenoviruses, we injected  $1 \times 10^9$  pfu into each tumor every 5 days (thrice in total) when the tumors were roughly 3 to 4 mm in diameter. We monitored tumor growth and animal survival after the first injection. The tumors treated with the adenovirus expressing either AP-2 $\alpha$  or AP-2 $\gamma$  grew more slowly compared with vector control-treated and untreated tumors (Figure 6B). Better survival fractions were observed in AP-2-treated animals (data not shown).

## Discussion

There are many proteins and redundant pathways to protect cells from tumor formation. Besides p53, Rb, p16, and others, AP-2 $\alpha$  and AP-2 $\gamma$  are also implicated in tumor suppression. AP-2 $\alpha$  and AP-2 $\gamma$ , two members of the AP-2 family, are transcription factors with high homology to each other. AP-2 $\alpha$  and AP-2 $\gamma$  were shown to have some similar behaviors, including interaction with p53 [22,40], susceptibility to tumor necrosis factor- $\alpha$  downregulation [21], and neural development [4,8,9,41]. It has been reported that the AP-2 $\alpha$  transcription factor can upregulate p21, arrest cell cycle progression, induce apoptosis, and promote tumor death [20,33,42]. Moreover, both AP-2 $\alpha$  and AP-2 $\gamma$  are transcriptional targets of wt p53 [35]. Therefore, it has been suggested that not only AP-2 $\alpha$  but also AP-2 $\gamma$  have tumor-suppressor activities. In these studies, we have identified both AP-2 $\alpha$  and AP-2 $\gamma$  as transcription factors that inhibit MDA MB-231 cell growth *in vivo* and *in vitro*. Both AP-2 proteins can upregulate p21 mRNA and protein levels, arrest cell cycle in G<sub>1</sub>/G<sub>0</sub> phase, decrease tumor cell clonogenicity, downregulate cyclin D1 mRNA and protein levels, decrease Rb phosphorylation, and attenuate E2F function. Cell cycle arrest caused by AP-2 expression is attributed to tumor cell growth inhibition *in vivo* and *in vitro*. We further demonstrated that p21 is the mediator, at least in part, between AP-2 and cell cycle regulation by using HCT116 parental and p21 (–/–) cells. The failure to induce cell cycle arrest in

G<sub>1</sub>/G<sub>0</sub> phase and to decrease BrdU incorporation by AP-2 in HCT116 p21 (–/–) cells revealed the importance of p21 as an AP-2 downstream target in cell cycle modulation. AP-2 $\alpha$  and AP-2 $\gamma$  appear to act in the same fashion in regard to cell cycle regulation and p21 elevation.

AP-2 $\alpha$  expression predicts survival in melanoma and breast cancer [27,42]. Some *in vivo* studies showed elevated melanoma growth by inactivating AP-2 $\alpha$  expression [42]. Here, we demonstrated decreased tumorigenicity of MDA MB-231 cells in nude mice after adenoviral AP-2 $\alpha$  or AP-2 $\gamma$  infection, and corresponding animal survival was greatly improved. To determine the role of AP-2 in cancer treatment, we infected established tumors with the same doses of adenoviruses, and decreased tumor growth was observed in AP-2-treated groups in comparison with untreated and vector control-treated groups. Thus, it would be desirable to develop therapeutic strategies aimed at breast cancer based on targeted reexpression of AP-2 $\alpha$  and/or AP-2 $\gamma$ .

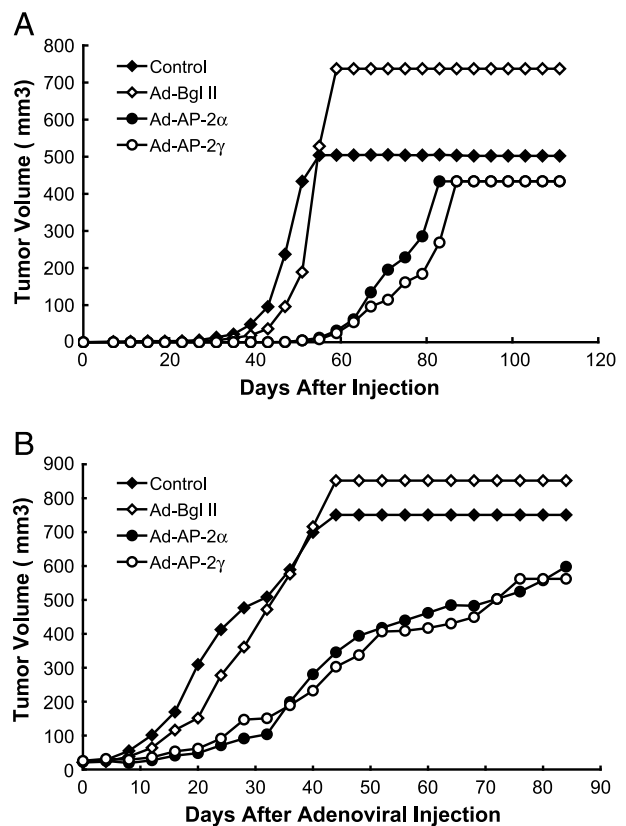


**Figure 6.** AP-2-expressing MDA MB-231 cells showed less tumorigenicity, and adenoviral AP-2 infection significantly delayed established tumor growth *in vivo*. (A) MDA MB-231 cells were infected with 100 MOI of vector control or Ad-AP-2 *in vitro* for 24 hours before injection. Under sterile conditions, 7- to 8-week-old nude mice were injected subcutaneously (day 0). Tumor sizes were measured and calculated according to the description in the Materials and Methods section. For statistical analysis, time of tumor initiation was defined as the first day on which tumor volume exceeded 10 mm<sup>3</sup>. (B) Under sterile conditions, 7- to 8-week-old nude mice were injected subcutaneously with MDA MB-231 cells. When the average diameter reached 3 to 4 mm, animals were grouped to achieve the same average tumor volume per group. Then  $1 \times 10^9$  pfu of indicated adenoviruses was injected into each tumor (day 0). Adenoviral injections (a total of three injections) were performed every 5 days. Animals were sacrificed when any tumor reached 1000 mm<sup>3</sup> in either flank. \**P* < .05 compared to untreated and Ad-Bgl II-treated groups.



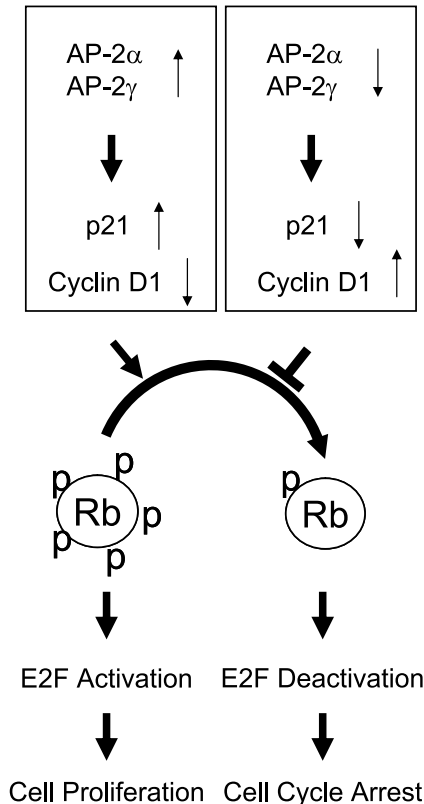


**Figure 7.** A proposed model for cell growth inhibition by AP-2 $\alpha$  and AP-2 $\gamma$ . In the presence of overexpressed wt AP-2 $\alpha$  or AP-2 $\gamma$ , p21 mRNA and proteins are present at high levels, whereas cyclin D1 expression is inhibited. The consequent pRb hypophosphorylation leads to E2F inactivation, which facilitates cell cycle arrest. When AP-2 $\alpha$  or AP-2 $\gamma$  expression is lost, such as during tumor formation, p21 expression is also lost and cyclin D1 becomes more actively expressed. The subsequent phosphorylation of pRb and activation of E2F promote cell proliferation and tumor formation.

Based on our findings, we propose a model for the mechanisms involved in AP-2–induced cell growth inhibition (Figure 7). In the presence of wt AP-2 $\alpha$  or AP-2 $\gamma$ , p21 mRNA and proteins are expressed, whereas cyclin D1 is repressed. Consequent pRb hypophosphorylation leads to E2F inactivation, which facilitates cell cycle arrest. When AP-2 $\alpha$  or AP-2 $\gamma$  expression is lost during tumor formation, p21 expression is decreased and cyclin D1 becomes more actively expressed. The subsequent phosphorylation of pRb and activation of E2F promote cell proliferation and tumor formation.

In the current study, the mechanisms involved in AP-2–induced p21 upregulation were investigated. A previous study by Zeng et al. [33] identified a 20-bp sequence consisting of three AP-2–binding sites located at the proximal p21 promoter as AP-2 $\alpha$ –responsive elements. Because both AP-2 $\alpha$  and AP-2 $\gamma$  bind to the same consensus-binding sites, we demonstrated that both AP-2 can bind to the p21 proximal promoter *in vivo*. It is reasonable that AP-2 $\alpha$  and AP-2 $\gamma$  work together to upregulate p21. Our previous study showed that AP-2 $\alpha$  and AP-2 $\gamma$  act synergistically to transactivate a 12 $\times$  AP-2–responsive CAT reporter [35]. Whether AP-2 family members work synergistically to regulate p21 and cell cycle control needs further investigation.

Besides the tumor-suppressor effects of AP-2, it also plays a very important and indispensable role in development and differentiation [43,44]. AP-2 $\alpha$  knockout mice have lethal defects and usually die at birth [43]. Moreover, some differentiated tissues retain AP-2 $\alpha$  expression after development. It is suggested that AP-2 $\alpha$  keep these cells from uncontrolled division after an appropriate physiological growth stimulus. Different members from the AP-2 family may play variable roles in different stages throughout life.

Future work will seek to identify different functions among AP-2 family members and further examine whether both AP-2 $\gamma$  with AP-2 $\alpha$  can work synergistically as therapeutic genes to improve cancer therapy or survival. Overall, this study compared AP-2 $\gamma$  with AP-2 $\alpha$  in suppressing certain aspects of the malignant phenotype. Our results indicate that AP-2 $\gamma$  binds to the p21 promoter *in vivo*, activates its expression, and thus causally participates in cell cycle arrest in human carcinoma cells derived from the breast and the colon. Our results further suggest that both AP-2 $\gamma$  with AP-2 $\alpha$  can inhibit tumor growth and therefore serve as tumor suppressors.

#### Acknowledgements

We thank the Gene Transfer Vector Core Facility of the University of Iowa Center for Gene Therapy of Cystic Fibrosis and Other Genetic Diseases (supported by NIH/NIDDK P30 DK 54759) for manufacturing the adenoviruses; the University of Iowa Flow Cytometry Facility for performing cell cycle analysis; Bert Vogelstein and Ronald Weigel for providing valuable constructs and materials; Dawn Quelle and Frederick Quelle for expert assistance with pRb Western blot analysis; Lei Yu for designing p21 ChIP primers; and Brian Smith for statistical analysis of animal data.

#### References

- [1] Mitchell PJ, Wang C, and Tjian R (1987). Positive and negative regulation of transcription *in vitro*: enhancer-binding protein AP-2 is inhibited by SV40T antigen. *Cell* **50**, 847–861.
- [2] Williams T, Admon A, Luscher B, and Tjian R (1988). Cloning and expression of AP-2, a cell-type–specific transcription factor that activates inducible enhancer elements. *Genes Dev* **2**, 1557–1569.
- [3] Moser M, Imhof A, Pscherer A, Bauer R, Amselgruber W, Sinowatz F, Hofstadter F, Schule R, and Buettner R (1995). Cloning and characterization of a second AP-2 transcription factor: AP-2 beta. *Development* **121**, 2779–2788.
- [4] Chazaud C, Oulad-Abdelghani M, Bouillet P, Decimo D, Chambon P, and Dolle P (1996). AP-2.2, a novel gene related to AP-2, is expressed in the forebrain, limbs and face during mouse embryogenesis. *Mech Dev* **54**, 83–94.
- [5] Zhao F, Satoda M, Licht JD, Hayashizaki Y, and Gelb BD (2001). Cloning and characterization of a novel mouse AP-2 transcription factor, AP-2delta, with unique DNA binding and transactivation properties. *J Biol Chem* **276**, 40755–40760.
- [6] Tummala R, Romano R-A, Fuchs E, and Sinha S (2003). Molecular cloning and characterization of AP-2 epsilon, a fifth member of the AP-2 family. *Gene* **321**, 93–102.
- [7] Williams T and Tjian R (1991). Characterization of a dimerization motif in AP-2 and its function in heterologous DNA-binding proteins. *Science* **251**, 1067–1071.
- [8] Zhang J, Hagopian-Donaldson S, Serbedzija G, Elsemore J, Plehn-Dujowich D, McMahon AP, Flavell RA, and Williams T (1996). Neural tube, skeletal and body wall defects in mice lacking transcription factor AP-2. *Nature* **381**, 238–241.

- [9] Schorle H, Meier P, Buchert M, Jaenisch R, and Mitchell PJ (1996). Transcription factor AP-2 essential for cranial closure and craniofacial development. *Nature* **381**, 235–238.
- [10] West-Mays JA, Zhang J, Nottoli T, Hagopian-Donaldson S, Libby D, Strissel KJ, and Williams T (1999). AP-2 alpha transcription factor is required for early morphogenesis of the lens vesicle. *Dev Biol* **206**, 46–62.
- [11] Nottoli T, Hagopian-Donaldson S, Zhang J, Perkins A, and Williams T (1998). AP-2–null cells disrupt morphogenesis of the eye, face, and limbs in chimeric mice. *PNAS* **95**, 13714–13719.
- [12] Auman HJ, Nottoli T, Lakiza O, Winger Q, Donaldson S, and Williams T (2002). Transcription factor AP-2 gamma is essential in the extra-embryonic lineages for early postimplantation development. *Development* **129**, 2733–2747.
- [13] Huang S, Jean D, Luca M, Tainsky MA, and Bar-Eli M (1998). Loss of AP-2 results in downregulation of c-kit and enhancement of melanoma tumorigenicity and metastasis. *EMBO J* **17**, 4358–4369.
- [14] Jean D, Gershenwald JE, Huang S, Luca M, Hudson MJ, Tainsky MA, and Bar-Eli M (1998). Loss of AP-2 results in up-regulation of MCAM/MUC18 and an increase in tumor growth and metastasis of human melanoma cells. *J Biol Chem* **273**, 16501–16508.
- [15] Bar-Eli M (1999). Role of AP-2 in tumor growth and metastasis of human melanoma. *Cancer Metastasis Rev* **18**, 377–385.
- [16] Marreiros A, Czolij R, Yardley G, Crossley M, and Jackson P (2003). Identification of regulatory regions within the KAI1 promoter: a role for binding of AP1, AP2 and p53. *Gene* **302**, 155–164.
- [17] Turner B, Zhang J, Gumbs A, Maher M, Kaplan L, Carter D, Glazer P, Hurst H, Haffty B, and Williams T (1998). Expression of AP-2 transcription factors in human breast cancer correlates with the regulation of multiple growth factor signalling pathways. *Cancer Res* **58**, 5466–5472.
- [18] Zhu C-H and Domann FE (2002). Dominant negative interference of transcription factor AP-2 causes inhibition of REBB-3 expression and suppresses malignant cell growth. *Breast Cancer Res Treat* **71**, 47–57.
- [19] McPherson L and Weigel R (1999). AP-2 alpha and AP-2 gamma: a comparison of binding site specificity and trans-activation of the estrogen receptor promoter and single site promoter constructs. *Nucleic Acids Res* **27**, 4040–4049.
- [20] Wajapeyee N and Somasundaram K (2003). Cell cycle arrest and apoptosis induction by activator protein 2 alpha and the role of p53 and p21WAF1/CIP1 in AP-2 alpha–mediated growth inhibition. *J Biol Chem* **278**, 52093–52101.
- [21] Nyormoi O, Wang Z, Doan D, Ruiz M, McConkey D, and Bar-Eli M (2001). Transcription factor AP-2(alpha) is preferentially cleaved by caspase 6 and degraded by proteasome during tumor necrosis factor alpha–induced apoptosis in breast cancer cells. *Mol Cell Biol* **21**, 4856–4867.
- [22] McPherson LA, Loktev AV, and Weigel RJ (2002). Tumor suppressor activity of AP-2 alpha mediated through a direct interaction with p53. *J Biol Chem* **277**, 45028–45033.
- [23] Wu F and Lee A (1998). Identification of AP-2 as an interactive target of RB and a regulator of the G1/S control element of the hamster histone H3.2 promoter. *Nucleic Acids Res* **26**, 4837–4845.
- [24] Batsche E, Muchardt C, Behrens J, Hurst HC, and Cremisi C (1998). Rb and c-myc activate expression of the *E-cadherin* gene in epithelial cells through interaction with transcription factor AP-2. *Mol Cell Biol* **18**, 3647–3658.
- [25] Ruiz M, Pettaway C, Song R, Stoeltz O, Ellis L, and Bar-Eli M (2004). Activator protein 2 alpha inhibits tumorigenicity and represses vascular endothelial growth factor transcription in prostate cancer cells. *Cancer Res* **64**, 631–638.
- [26] Mitchell DC, Abdelrahim M, Weng J, Stafford LJ, Safe S, Bar-Eli M, and Liu M (2006). Regulation of *KiSS-1* metastasis suppressor gene expression in breast cancer cells by direct interaction of transcription factors activator protein-2 alpha and specificity protein-1. *J Biol Chem* **281**, 51–58.
- [27] Pellikainen J, Kataja V, Ropponen K, Kellokoski J, Pietilainen T, Bohm J, Eskelinen M, and Kosma V-M (2002). Reduced nuclear expression of transcription factor AP-2 associates with aggressive breast cancer. *Clin Cancer Res* **8**, 3487–3495.
- [28] Gee JMW, Robertson JFR, Ellis IO, Nicholson RI, and Hurst HC (2000). Immunohistochemical analysis reveals a tumour suppressor–like role for the transcription factor AP-2 in invasive breast cancer. *J Pathol* **189**, 514–520.
- [29] Douglas DB, Akiyama Y, Carraway H, Belinsky SA, Esteller M, Gabrielson E, Weitzman S, Williams T, Herman JG, and Baylin SB (2004). Hypermethylation of a small CpGuanine-rich region correlates with loss of activator protein-2 alpha expression during progression of breast cancer. *Cancer Res* **64**, 1611–1620.
- [30] Hoei-Hansen CE, Nielsen JE, Almstrup K, Sonne SB, Graem N, Skakkebaek NE, Leffers H, and Meyts ER-D (2004). Transcription factor AP-2gamma is a developmentally regulated marker of testicular carcinoma *in situ* and germ cell tumors. *Clin Cancer Res* **10**, 8521–8530.
- [31] Pauls K, Jager R, Weber S, Wardelmann E, Koch A, Buttner R, and Schorle H (2005). Transcription factor AP-2gamma, a novel marker of gonocytes and seminomatous germ cell tumors. *Int J Cancer* **115**, 470–477.
- [32] Jager R, Friedrichs N, Heim I, Buttner R, and Schorle H (2005). Dual role of AP-2 gamma in ERBB-2–induced mammary tumorigenesis. *Breast Cancer Res Treat* **90**, 273–280.
- [33] Zeng YX, Somasundaram K, and el-Deiry WS (1997). AP-2 inhibits cancer cell growth and activates p21WAF1/CIP1 expression. *Nat Genet* **15**, 78–82.
- [34] Zhu C-H, Huang Y, Oberley LW, and Domann FE (2001). A family of AP-2 proteins down-regulate manganese superoxide dismutase expression. *J Biol Chem* **276**, 14407–14413.
- [35] Li H, Watts GS, Oshiro MM, Futscher BW, and Domann FE (2006). AP-2 alpha and AP-2 gamma are transcriptional targets of p53 in human breast carcinoma cells. *Oncogene* (in press). DOI: 10.1038/sj.onc.1209534. PM ID:16636674
- [36] Buckley MF, Sweeney KJ, Hamilton JA, Sini RL, Manning DL, Nicholson RI, deFazio A, Watts CK, Musgrove EA, and Sutherland RL (1993). Expression and amplification of cyclin genes in human breast cancer. *Oncogene* **8**, 2127–2133.
- [37] Bartkova J, Lukas J, Muller H, Lutzhoft D, Strauss M, and Bartek J (1994). Cyclin D1 protein expression and function in human breast cancer. *Int J Cancer* **57**, 353–361.
- [38] Fu M, Wang C, Li Z, Sakamaki T, and Pestell RG (2004). Cyclin D1: normal and abnormal functions [minireview]. *Endocrinology* **145**, 5439–5447.
- [39] Weinberg RA (1995). The retinoblastoma protein and cell cycle control. *Cell* **81**, 323–330.
- [40] Modugno M, Tagliabue E, Ardini E, Berno V, Galmozzi E, Bortoli MD, Castronovo V, and Menard S (2002). p53-dependent downregulation of metastasis-associated laminin receptor. *Nature* **21**, 7478–7487.
- [41] Werling U and Schorle H (2002). Transcription factor gene AP-2-(gamma) essential for early murine development. *Mol Cell Biol* **22**, 3149–3156.
- [42] Bar-Eli M (2001). Gene regulation in melanoma progression by the AP-2 transcription factor. *Pigment Cell Res* **14**, 78–85.
- [43] Hilger-Eversheim K, Moser M, Schorle H, and Buettner R (2000). Regulatory roles of AP-2 transcription factors in vertebrate development, apoptosis and cell-cycle control. *Gene* **260**, 1–12.
- [44] Paggi MG, Bonetto F, Severino A, Baldi A, Battista T, Bucci F, Felsani A, Lombardi D, and Giordano A (2001). The retinoblastoma-related *RB2/p130* gene is an effector downstream of AP-2 during neural differentiation. *Oncogene* **20**, 2570–2578.